PHYSICAL REVIEW B **88**, 121301(R) (2013)

Strain tuning of optical emission energy and polarization in monolayer and bilayer MoS_2

C. R. Zhu,[1] G. Wang,[1] B. L. Liu,[1,†] X. Marie,[2] X. F. Qiao,[3] X. Zhang,[3] X. X. Wu,[1] H. Fan,[1] P. H. Tan,[3] T. Amand,[2] and B. Urbaszek[2,*]

[1]*Beijing National Laboratory for Condensed Matter Physics, Institute of Physics, Chinese Academy of Sciences, Beijing 100190, China*

[2]*Université de Toulouse, INSA-CNRS-UPS, LPCNO, 135 Avenue de Rangueil, 31077 Toulouse, France*

[3]*State Key Laboratory of Superlattices and Microstructures, Institute of Semiconductors, Chinese Academy of Sciences, Beijing 100083, China*

(Received 14 June 2013; revised manuscript received 4 August 2013; published 9 September 2013)

We use micro-Raman and photoluminescence (PL) spectroscopy at 300 K to investigate the influence of uniaxial tensile strain on the vibrational and optoelectronic properties of monolayer and bilayer MoS_2 on a flexible substrate. The initially degenerate E' monolayer Raman mode is split into a doublet as a direct consequence of the strain applied to MoS_2 through Van der Waals coupling at the sample-substrate interface. We observe a strong shift of the direct band gap of 48 meV/(% of strain) for the monolayer and 46 meV/% for the bilayer, whose indirect gap shifts by 86 meV/%. We find a strong decrease of the PL polarization linked to optical valley initialization for both monolayer and bilayer samples, indicating that scattering to the spin-degenerate Γ valley plays a key role.

DOI: 10.1103/PhysRevB.88.121301 PACS number(s): 78.60.Lc, 78.66.Li

I. INTRODUCTION

Transition-metal dichalcogenides such as MoS_2 emerge as an exciting class of atomically flat, two-dimensional materials for electronics and optoelectronics. In contrast to graphene, monolayer MoS_2 has a direct band gap[1,2] in the visible region of the optical spectrum and has been used as the active region of field-effect transistors,[3] complex electronic circuits,[4] and light-emitting diodes.[5] Another important difference to graphene is the broken inversion symmetry of monolayer MoS_2, which can be directly used for second harmonic generation in nonlinear optics.[6] The combined presence of inversion symmetry breaking and strong spin-orbit coupling[7–9] allows simple optical k-valley initialization with circularly polarized lasers.[10–13] This opens up very exciting possibilities of manipulating carriers in valleys with contrasting Berry phase curvatures,[14] which allows in principle the observation of the valley Hall effect.[15] The valley and spin properties are closely linked to the crystal symmetry and are expected to be modified through the application of mechanical strain. The role of strain is also important for practical devices using MoS_2 on flexible substrates. In unstrained samples, the indirect band gap of monolayer MoS_2 is just above the direct band gap.[2,7,16] Strain will therefore have important consequences as the indirect transition approaches the direct transition energy before monolayer MoS_2 becomes indirect for strain exceeding 1.5%.[17]

Here we apply a relatively small tensile uniaxial strain of up to 0.8% to observe striking changes in the Raman spectra of monolayers and bilayers. Drastic changes in optical emission properties are observed: the band gap is shifted by several tens of meV and the PL polarization changes by 40% for the monolayer and 100% for the bilayer (i.e., the finite PL polarization is tuned to zero). These results suggest that scattering to the spin-degenerate Γ valley[7] plays a key role as it becomes more efficient as strain increases.

II. SAMPLES AND SETUP

To controllably induce strain, the MoS_2 flakes are obtained by micromechanical exfoliation of natural bulk MoS_2 crystals (SPI Supplies, West Chester, PA) onto a flexible substrate, which is a polyethylene terephthalate (PET) film (9 cm long, 1 cm wide, 1 mm thick). The MoS_2 flakes remain at a fixed position on the substrate due to van der Waals attraction. Uniaxial strain is applied to MoS_2 through bending the PET film in a three-point apparatus (the distance between two extreme points is 6 cm). To achieve maximum strain, the MoS_2 flake is positioned exactly on top of the center point; see Fig. 1(b). The induced strain ϵ is given by $\epsilon = t/2R$, where $t = 1$ mm is the thickness of PET film and R is the radius of curvature of the bent substrate. R is evaluated by measuring the displacement of the central point of the substrate (i.e., where the strain is applied). The angle at which the strain is applied with respect to the MoS_2 in-plane crystal orientation can be adjusted as the bending apparatus is mounted on a rotation stage. Raman spectroscopy is performed in a backscattering geometry using a Jobin-Yvon HR800 Raman system equipped with a liquid-nitrogen-cooled charge-coupled device (CCD) and laser excitation at 2.6 eV. This allows us to verify that the MoS_2 flakes adhere well to the bent substrate during the measurements (i.e., no sample slippage occurs). Microphotoluminescence (PL) spectra are measured with a 100× long-working-distance objective using a He-Ne laser at 1.95 eV for excitation. The laser beam is passed through a Soleil Babinet Compensator to create circularly polarized light. The PL polarization P_c defined as $P_c = \frac{I_{\sigma+}-I_{\sigma-}}{I_{\sigma+}+I_{\sigma-}}$ is analyzed by a quarter-wave plate placed in front of a Glan-Thomson linear polarizer. Here $I_{\sigma+}$ ($I_{\sigma-}$) denotes the intensity of the σ^+ (σ^-) -polarized emission at the PL peak. All experiments are carried out at room temperature.

III. EXPERIMENTAL RESULTS

Before applying strain, the monolayer and bilayer regions are localized by micro-Raman spectroscopy.[18,19] The high-frequency Raman spectra of the unstrained monolayer and bilayer MoS_2 are, respectively, characterized by E' and A_1' (monolayer) and E^1_{2g} and A_{1g} (bilayer) due to their difference in symmetry (D_{3h} for monolayer and D_{6h} for bilayer),[20] as

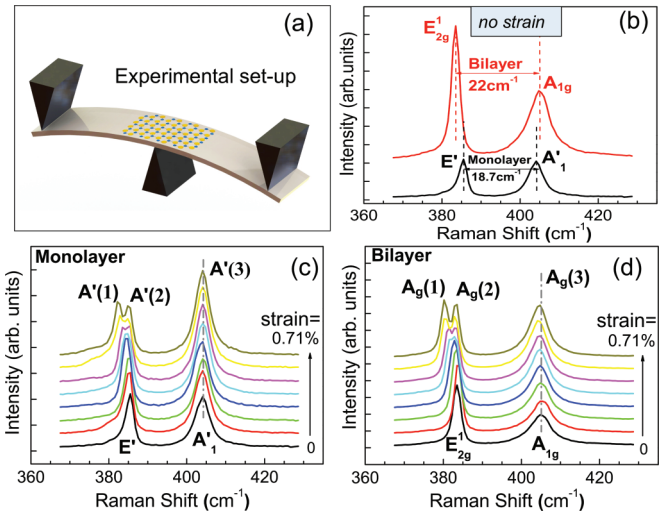

FIG. 1. (Color online) (a) The three-point bending apparatus. Note that the distance between the two top contact points is 6 cm, whereas the extension of a MoS_2 flake is in the μm range. (b) The monolayer (black curve) and bilayer (red) MoS_2 regions are identified by Raman spectroscopy. (c) The E' Raman mode splits into two modes as tensile strain is applied to the monolayer sample. (d) Same as (c) but for a bilayer sample.

shown in Fig. 1(b). The frequency difference between E' and A_1' in the monolayer (18.7 cm^{-1}) is smaller than that between E^1_{2g} and A_{1g} in the bilayer (22 cm^{-1}).[18] A_1' and A_{1g} reflect the vibration along the z axis, whereas E' and E^1_{2g} describe the vibration within the xy base plane. In the absence of strain, E' and E^1_{2g} are two-dimensional degenerate modes. As uniaxial strain is applied to the monolayer and bilayer, they split into two modes as the degeneracy is lifted, as shown in Figs. 1(c) and 1(d). The lattice symmetry of the monolayer and bilayer changes to C_s and C_{2h} under uniaxial strain, respectively. The Raman spectrum of the monolayer is characterized by three A' modes, while that of the bilayer is characterized by three A_g modes. With increasing tensile strain applied to the monolayer, the frequency shift is very small for the $A'(3)$ mode, indicating that the tensile strain has little effect on the vibration perpendicular to the xy plane. However, the E' mode in the unstrained monolayer splits into two modes [$A'(1)$ and $A'(2)$] in the strained monolayer. The larger frequency shift of the $A'(1)$ mode with strain signifies that $A'(1)$ vibrates along the direction of the tensile strain. Similar results are also observed in the strained bilayer. In a recent report, only a broadening, not a splitting of the E' mode, has been observed for a monolayer,[21] which may be due to a lower spectral resolution. The splitting of the E' mode in the monolayer and the E^1_{2g} mode in the bilayer clearly shows that strain is successfully applied to the samples via van der Waals force at the substrate sample interface. The applied strain is limited to 0.8% to avoid sample slippage.[22]

In Fig. 2(a) we present the PL emission of a typical monolayer sample excited with a σ^+ circularly polarized laser. We detect a circular polarization degree in the order of 10% due to the chiral optical selection rules in MoS_2 monolayers[10,15] linked to K-valley polarization.[11–13,23] As the strain is increased up to 0.8%, we observe two striking

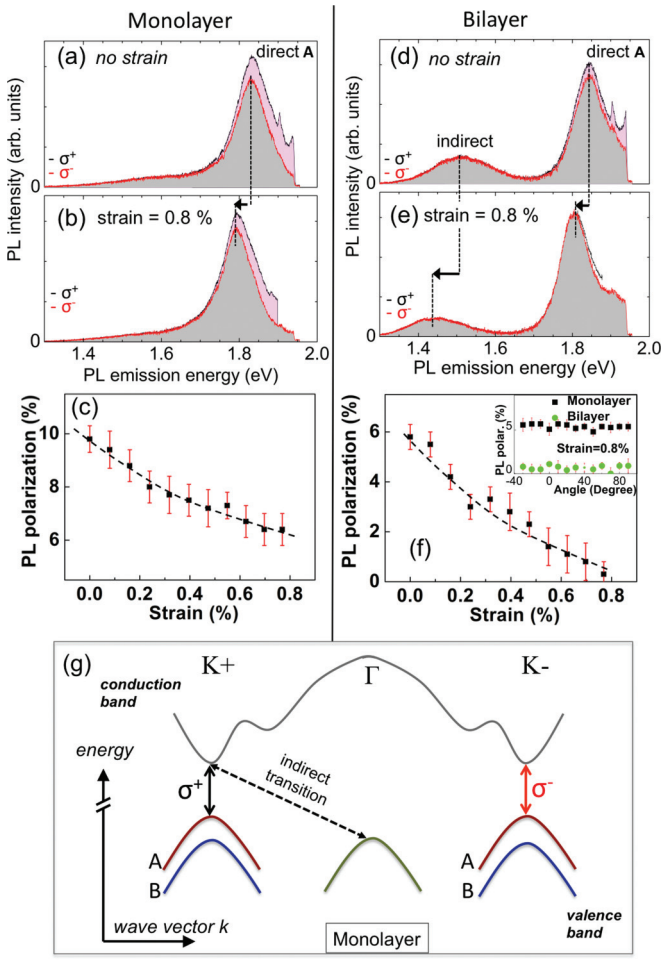

FIG. 2. (Color online) Laser excitation at 1.95 eV with σ^+ polarization. (a) PL emission detected for σ^+ and σ^- polarization for a MoS_2 monolayer at zero strain. (b) Same as (a) but for applied strain of 0.8%. (c) Circular polarization degree of the PL detected at its peak as a function of the applied tensile strain. Dotted lines are a guide to the eye. (d) PL emission detected for σ^+ and σ^- polarization for a MoS_2 bilayer at zero strain. (e) Same as (d) but for applied strain of 0.8%. (f) PL Circular polarization degree as a function of the applied tensile strain. Dotted lines are guides to the eye. Inset: The applied strain is kept constant at 0.8% and the PL polarization is measured as a function of the angle of the applied strain with respect to the in-plane mono- and bilayer crystal orientation. (g) Scheme of the band structure for monolayer MoS_2 at zero strain. K and Γ valleys and the associated interband transitions are marked; the conduction-band spin splitting in the meV range[7] is not shown.

changes in Fig. 2(b): First, the emission is shifted by several tens of meV to lower energy. Second, the PL polarization degree P_c decreases. This is confirmed in Fig. 2(c), where we measure a systematic decrease of P_c with increasing strain.

Also for the bilayer sample we observe a shift of the PL emission energy associated with the direct transition; compare Figs. 2(d) and 2(e). This emission is polarized in the absence of strain to about 6%. Note that the PL polarization of the indirect optical transitions at lower energy is zero, as expected (see also the discussion below). Under the maximum tensile strain of 0.8%, the PL polarization of both transitions (direct

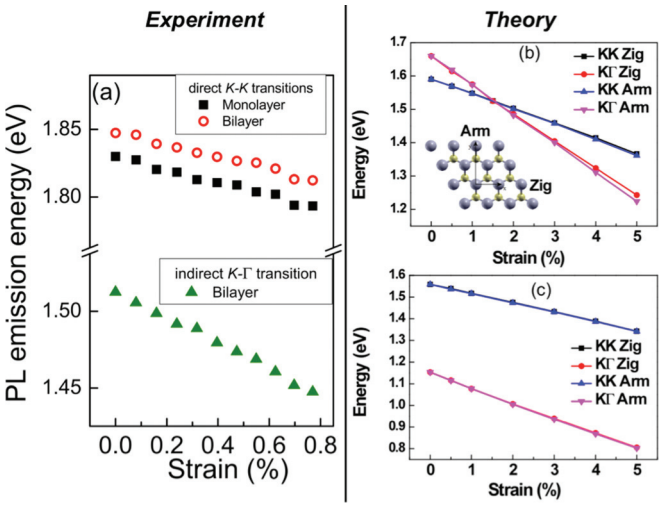

FIG. 3. (Color online) (a) Measured energy shift for the direct recombination of the MoS_2 monolayer (squares) and bilayer sample (circles), and indirect recombination for the bilayer (triangles) for applied strain between 0% and 0.8%. (b) Calculation (see the main text) of the evolution of the direct and indirect band gap for a MoS_2 monolayer with strain from 0% to 5% applied along the zigzag and armchair directions. (c) Same as (b) but for a MoS_2 bilayer.

and indirect) is zero and they are shifted to lower energy in Fig. 2(e). We observe that P_c for the bilayer can be tuned continuously from 6% to zero as strain is increased in Fig. 2(f). By rotating the sample, we have verified that the decrease in polarization does not depend on the direction of the tensile strain applied in the plane [see the inset of Fig. 2(f)],[24] in good agreement with our calculations presented in Figs. 3(b) and 3(c).

The systematically measured shift in PL emission energy due to a strain-induced reduction in band gap is plotted in Fig. 3(a). We observe a strong shift of the *direct* band gap of 48 meV/% of strain for the monolayer and 46 meV/% for the bilayer. The shift of the *indirect* gap of the bilayer of 86 meV/% is nearly twice as high. These shifts are in agreement with our calculations and the calculations reported in the literature; see, for example, Refs. 17,25–27. Our density functional theory (DFT) calculations employ the projector augmented wave (PAW) method encoded in the Vienna *ab initio* simulation package (VASP),[28–30] and the Perdew-Burke-Ernzerhof (PBE) exchange correlation functional[31] is used. Throughout this work, a cutoff energy of 400 eV is taken for expanding the wave functions into the plane-wave basis. For the relaxation of bilayer MoS_2, the long-range van der Waals interaction is accounted for by means of a semiempirical DFT-D2 approach proposed by Grimme.[32] The calculated parameters for monolayer and bilayer MoS_2 are $a = 3.189$ Å and 3.196 Å with $15 \times 15 \times 1$ Γ centered k-point grids. A 20 Å vacuum layer is used in our calculation to avoid interactions between slabs. The convergence for energy is chosen as 10^{-5} eV between two steps, and the maximum Hellmann-Feynman force acting on each atom is less than 0.01 eV/Å upon ionic relaxation. Figure 3(b) shows the evolution of the calculated band gap with strain using the PBE functional. Although the band gap is underestimated, the calculated shift of the direct band gap is 42 meV/% for the monolayer and bilayer and the shift of the indirect band gap is 76 meV/% for the bilayer, which is in good agreement with our experimental observation. Our calculations expect a crossing of a direct and indirect band gap at $\epsilon = 1.5\%$, in agreement with the prediction of Shi *et al.*,[17] which we cannot verify directly in our experiment as the applied strain is limited to $\epsilon = 0.8\%$.

IV. DISCUSSION

For a relatively small uniaxial strain amplitude, we observe profound changes in the electronic structure of monolayer and bilayer MoS_2. We first analyze the observations for the monolayer sample.

Monolayer MoS_2 has a direct band gap at the K point with chiral optical selection rules,[10,15] see Fig. 2(g). When a laser is resonant with the **A** valence band ($K^{\pm}$ valley) to the conduction-band transition, σ^+-polarized light will result in the creation of a conduction electron in the K_c^+ valley, while σ^--polarized light creates a K_c^- electron. In emission, the same selection rules apply, so in the absence of intervalley carrier transfer (and spin flips) the emission is expected to be strongly polarized, as is observed at low temperature.[10–13] The valley and spin states are less stable and less well defined at room temperature, and lower PL polarization degrees are observed as also reported here. In our experiments, the exciting photon energy is close to the **B** K valence- to conduction-band transition. As a result, both **B** and **A** bands are excited due to energy broadening by impurities, phonons, and substrate imperfections.[23,33] The B excitons have to relax in energy, which can lead to a change in valley if high k-value phonons are emitted.

It is important to note that although the fundamental gap of monolayer MoS_2 is direct, the indirect gap between the valence-band maximum Γ_v and the degenerate conduction-band minima K_c^+ and K_c^- is very close in energy,[16] as indicated in Fig. 2(g). This means that at room temperature, as energy levels are broadened and due to high phonon occupation numbers, the Γ_v states will play an important role in optics and transport, as has been theoretically predicted.[33,34] Although the phonon-assisted indirect absorption is a second-order process, it cannot be neglected since it has many more available final states compared with direct absorption.[35] The chiral optical selection rules that allow optical valley initialization do not apply to the $\Gamma_v \leftrightarrow K_c^{\pm}$ transitions.[7–9,16] Therefore, phonon-assisted light absorption and emission involving the Γ valence states will be essentially unpolarized.

As *strain* is applied to a *monolayer* sample, theory predicts that the $\Gamma_v \leftrightarrow K_c^{\pm}$ transition becomes the fundamental transition for $\epsilon > 1.5\%$; see our calculation in Fig. 3(b). So the impact of the indirect transitions on the optical properties will be more important the higher the strain is. The scattering to the spin-degenerate Γ valley could be at the origin of the observed decrease of the PL polarization of the **A** transition as a function of the applied strain [Fig. 2(c)]. As the strain is increased in our experiment, we do not move our laser energy, which is constant at 1.95 eV, although the band gap shifts to the red. In general, the more off-resonant the optical excitation, the lower the polarization on the ground state.[23]

We now discuss the observed lowering of the PL polarization of the *bilayer* with the applied strain. An ideal bilayer possesses inversion symmetry, and chiral valley selection rules do not apply.[9,10,15] For zero external strain, we observe a 6% PL polarization, so symmetry breaking due to surface and interface effects is likely (assuming fast electron and hole spin relaxation compared to the radiative lifetime). A nonzero bilayer PL polarization has been reported before.[11,36] Inversion symmetry breaking also manifests itself by second harmonic generation,[6] forbidden for a perfectly symmetrical bilayer. The bilayer emission is very rich in information due to the coexistence of indirect and direct emission: at zero strain, the direct optical emission is circularly polarized, whereas the indirect emission (unfortunately not detectable for the monolayer) is unpolarized in Fig. 2(d). The relative change in P_c in the bilayer (100%) is bigger than that in the monolayer (40%). This may be due to the fact that the indirect transition is already the fundamental band gap as we start the measurements at zero strain. As we keep our laser energy constant, we excite more and more nonresonantly as the strain increases. The application of strain could also partially restore inversion symmetry for the bilayer, which would contribute in addition to lowering the PL polarization.[36] The induced strain could also accelerate spin relaxation, similar to the observations in GaAs.[37] Also, the clear chiral optical selection rules derived for MoS_2 K-valley transitions will work less well as the applied strain modifies the direct band gap at K and the indirect ($\Gamma_v \leftrightarrow K_c^{\pm}$) band gap.[9]

V. CONCLUSION

The unique coexistence of direct and indirect exciton transitions in uniaxially strained MoS_2 monolayers and bilayers has been investigated in the context of valley polarization. For monolayers, this coexistence is very promising for p-type Gunn diodes in applied electric fields[33] and has to be investigated further for realistic valley Hall experiments. To apply a larger strain of a few percent in order to verify the direct to indirect band gap changeover, the sample will have to be clamped (fixed) to the substrate to avoid slippage. A stronger separation between K and Γ valence bands is expected for monolayer WSe_2,[7] another promising dichalcogenide material with a direct gap also in the visible range.[38] Strain tuning is also a promising approach for varying optical and vibrational properties in monolayer $MoSe_2$.[39,40]

Note added. Recently, we became aware of two preprints reporting similar results on Raman and band-gap shifts.[41,42]

ACKNOWLEDGMENTS

We acknowledge partial funding from the CAS Grant No. 2011T1J37; the National Basic Research program of China (Grants No. 2009CB930502, No. 2009CB929301, No. 2010CB922904) and the National Science Foundation of China [Grants No. 11174338, No. 10911130356(Spinman), No. 11225421, and No. 10934007]; Labex NEXT Project "Valley-hall", and ERC StG. OptoDNPcontrol (B.U).

*urbaszek@insa-toulouse.fr

†blliu@iphy.ac.cn

[1] K. F. Mak, C. Lee, J. Hone, J. Shan, and T. F. Heinz, Phys. Rev. Lett. **105**, 136805 (2010).

[2] A. Splendiani, L. Sun, Y. Zhang, T. Li, J. Kim, C.-Y. Chim, G. Galli, and F. Wang, Nano Lett. **10**, 1271 (2010).

[3] B. Radisavljevic, A. Radenovic, J. Brivio, V. Giacometti, and A. Kis, Nature. Nanotech. **6**, 147 (2011).

[4] H. Wang, L. Yu, Y. Lee, W. Fang, A. Hsu, P. Herring, M. Chin, M. Dubey, L. Li, J. Kong *et al.*, in *IEEE International Electron Devices Meeting (IEDM)* (IEEE, Piscataway, NJ, 2012), pp. 4.6.1–4.6.4.

[5] R. S. Sundaram, M. Engel, A. Lombardo, R. Krupke, A. C. Ferrari, Ph. Avouris, and M. Steiner, Nano Lett. **13**, 1416 (2013).

[6] N. Kumar, S. Najmaei, Q. Cui, F. Ceballos, P. M. Ajayan, J. Lou, and H. Zhao, Phys. Rev. B **87**, 161403 (2013).

[7] Z. Y. Zhu, Y. C. Cheng, and U. Schwingenschlögl, Phys. Rev. B **84**, 153402 (2011).

[8] F. Zhang, J. Jung, G. A. Fiete, Q. Niu, and A. H. MacDonald, Phys. Rev. Lett. **106**, 156801 (2011).

[9] X. Li, F. Zhang, and Q. Niu, Phys. Rev. Lett. **110**, 066803 (2013).

[10] T. Cao, G. Wang, W. Han, H. Ye, C. Zhu, J. Shi, Q. Niu, P. Tan, E. Wang, B. Liu *et al.*, Nat. Commun. **3**, 887 (2012).

[11] K. F. Mak, K. He, J. Shan, and T. F. Heinz, Nat. Nanotech. **7**, 494 (2012).

[12] H. Zeng, J. Dai, W. Yao, D. Xiao, and X. Cui, Nat. Nanotech. **7**, 490 (2012).

[13] G. Sallen, L. Bouet, X. Marie, G. Wang, C. R. Zhu, W. P. Han, Y. Lu, P. H. Tan, T. Amand, B. L. Liu *et al.*, Phys. Rev. B **86**, 081301 (2012).

[14] D. Xiao, M.-C. Chang, and Q. Niu, Rev. Mod. Phys. **82**, 1959 (2010).

[15] D. Xiao, G.-B. Liu, W. Feng, X. Xu, and W. Yao, Phys. Rev. Lett. **108**, 196802 (2012).

[16] T. Cheiwchanchamnangij and W. R. L. Lambrecht, Phys. Rev. B **85**, 205302 (2012).

[17] H. Shi, H. Pan, Y.-W. Zhang, and B. I. Yakobson, Phys. Rev. B **87**, 155304 (2013).

[18] C. Lee, H. Yan, L. E. Brus, T. F. Heinz, J. Hone, and S. Ryu, ACS Nano **4**, 2695 (2010).

[19] T. Korn, S. Heydrich, M. Hirmer, J. Schmutzler, and C. Schüller, Appl. Phys. Lett. **99**, 102109 (2011).

[20] X. Zhang, W. P. Han, J. B. Wu, S. Milana, Y. Lu, Q. Q. Li, A. C. Ferrari, and P. H. Tan, Phys. Rev. B **87**, 115413 (2013).

[21] C. Rice, R. J. Young, R. Zan, U. Bangert, D. Wolverson, T. Georgiou, R. Jalil, and K. S. Novoselov, Phys. Rev. B **87**, 081307 (2013).

[22] Our experiments are carried out in the elastic regime: For a given strain, we obtain the same results if the strain is varied from zero to 0.8% or from 0.8% to zero.

[23] G. Kioseoglou, A. T. Hanbicki, M. Currie, A. L. Friedman, D. Gunlycke, and B. T. Jonker, Appl. Phys. Lett. **101**, 221907 (2012).

[24] As MoS_2 has trigonal C_{3v} symmetry, it is enough to cover 120° to verify the isotropy.

[25]J. Feng, X. Qian, C.-W. Huang, and J. Li, Nat. Photon. **6**, 866 (2012).

[26]W. S. Yun, S. W. Han, S. C. Hong, I. G. Kim, and J. D. Lee, Phys. Rev. B **85**, 033305 (2012).

[27]Although exciton binding energies are large in this system they do not depend on strain in a first approximation.[17,25] Calculating band-gap shifts in a single-particle picture allows us to describe the essential features here.

[28]G. Kresse and J. Hafner, Phys. Rev. B **47**, 558 (1993).

[29]G. Kresse and J. Furthmüller, Phys. Rev. B **54**, 11169 (1996).

[30]G. Kresse and J. Furthmüller, Comput. Mater. Sci. **6**, 15 (1996).

[31]J. P. Perdew, K. Burke, and M. Ernzerhof, Phys. Rev. Lett. **77**, 3865 (1996).

[32]S. Grimme, J. Comput. Chem. **27**, 1787 (2006).

[33]Y. Song and H. Dery, Phys. Rev. Lett. **111**, 026601 (2013).

[34]A. Kormanyos *et al*., Phys. Rev. B **88**, 045416 (2013).

[35]R. J. Elliott, Phys. Rev. **108**, 1384 (1957).

[36]S. Wu, J. S. Ross, G.-B. Liu, G. Aivazian, A. Jones, Z. Fei, W. Zhu, D. Xiao, W. Yao, D. Cobden, and X. Xu, Nature Physics **9**, 149 (2013).

[37]D. J. English, P. G. Lagoudakis, R. T. Harley, P. S. Eldridge, J. Hübner, and M. Oestreich, Phys. Rev. B **84**, 155323 (2011).

[38]A. M. Jones, H. Yu, N. J. Ghimire, S. Wu, G. Aivazian, J. S. Ross, B. Zhao, J. Yan, D. G. Mandrus, D. Xiao, W. Yao, and X. Xu, Nature Nanotechnology (2013), doi: 10.1038/nnano.2013.151.

[39]S. Horzum, H. Sahin, S. Cahangirov, P. Cudazzo, A. Rubio, T. Serin, and F. M. Peeters, Phys. Rev. B **87**, 125415 (2013).

[40]S. Tongay, J. Zhou, C. Ataca, K. Lo, T. S. Matthews, J. Li, J. C. Grossman, and J. Wu, Nano Lett. **12**, 5576 (2012).

[41]H. J. Conley, B. Wang, J. I. Ziegler, R. F. Haglund, Jr., S. T. Pantelides, and K. I. Bolotin, Nano Lett. **13**, 3626 (2013).

[42]K. He *et al*., Nano Lett. **13**, 2931 (2013).